

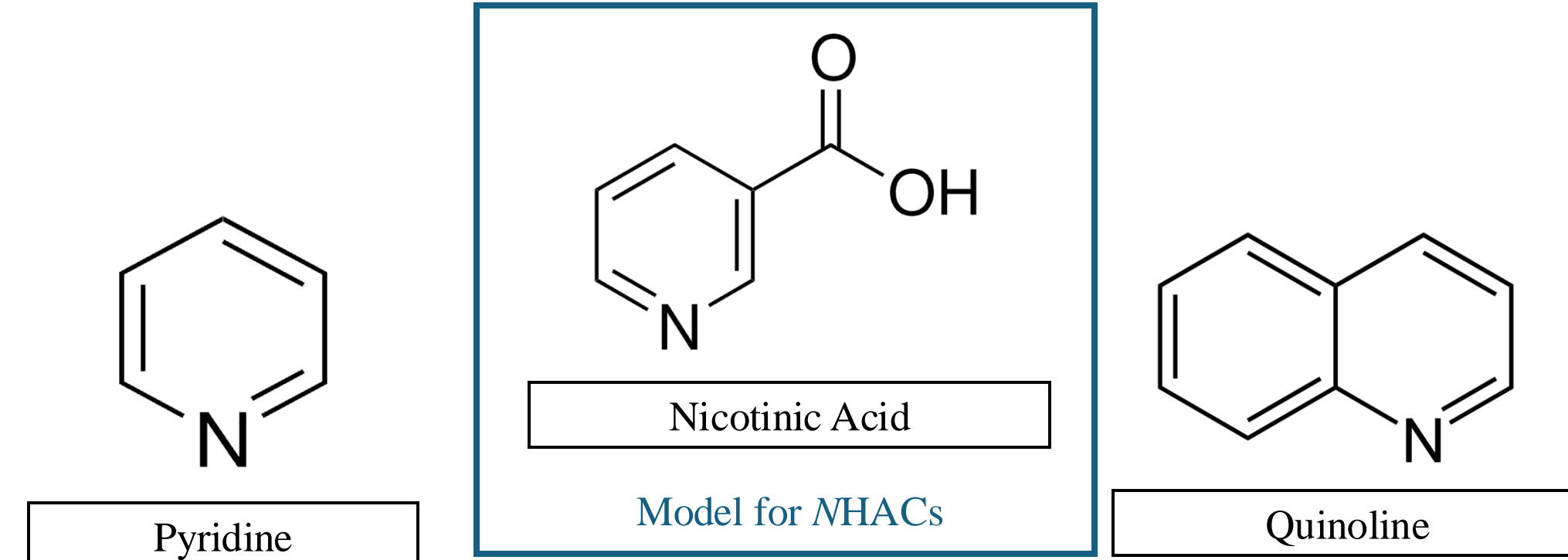
THE COLLEGE OF
WOOSTER

Investigating the Importance of Arg 108 in the Binding of NADH by NicC

Mayank R. Pandey and Mark J. Snider; Department of Biochemistry & Molecular Biology, The College of Wooster, Ohio

Background and Significance

- NHACs are prevalent in nature and are known to contaminate soils and groundwater, posing serious environmental and health risks, as they have been identified as carcinogenic¹ and toxic².
- Nicotinic acid is used as a model to study the biodegradation of NHACs.



Structure and Mechanism of NicC

- The two potential NADH binding sites in nicC: a larger site associated with FAD binding and a smaller site near the proposed 6-HNA entry channel.

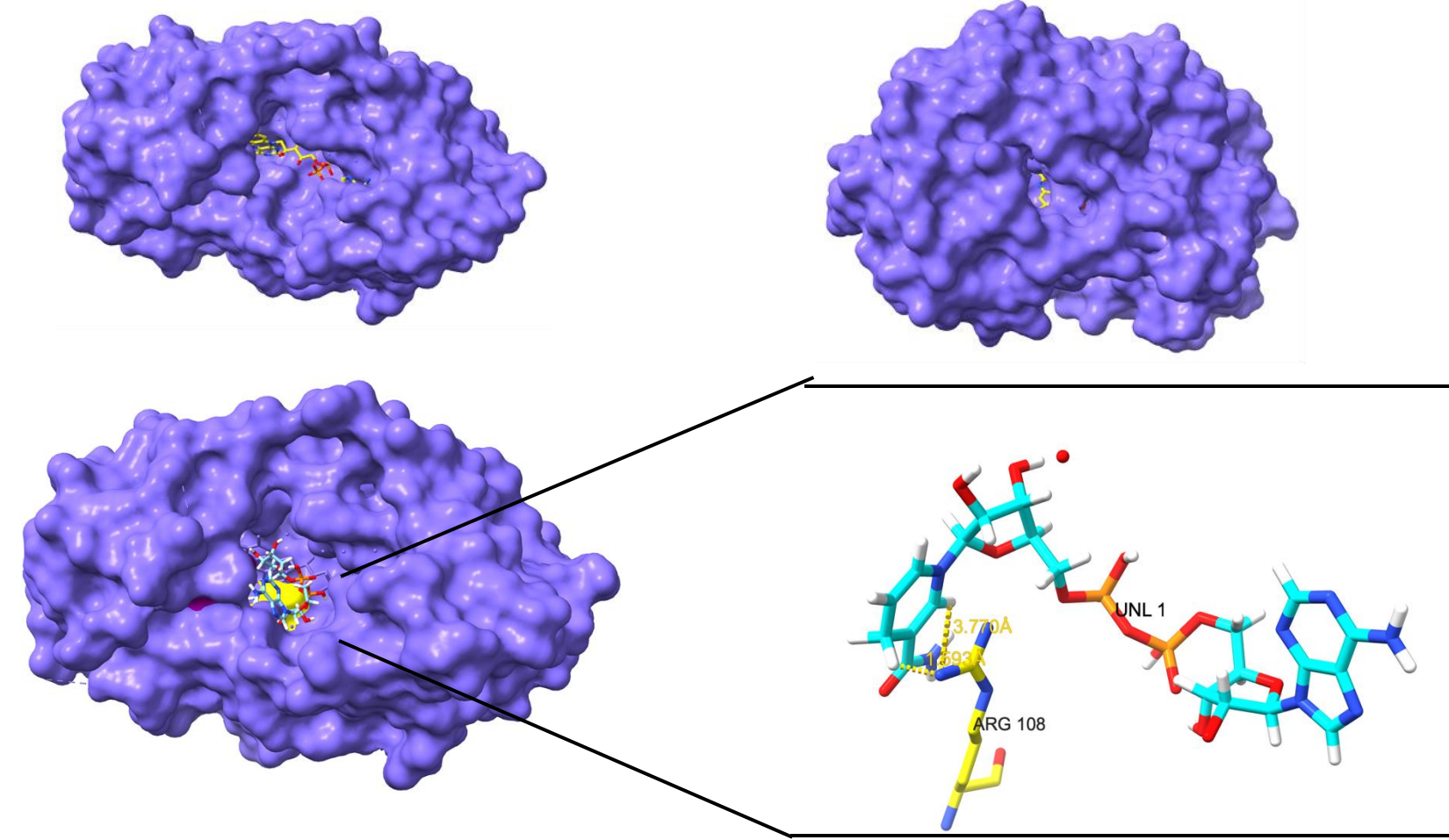


Figure 1. Potential interactions between NADH and key residues within nicC.

- This study hypothesizes that the FAD site heavily contributes to NADH recruitment and alignment. Additionally, the role of a residue within the FAD site is of particular interest, as it may be crucial for stabilizing NADH within the active site, potentially facilitating optimal electron transfer.

- Nicotinic acid's degradation pathway serves as a model for understanding the biodegradation of *N*-heterocyclic aromatic compounds.

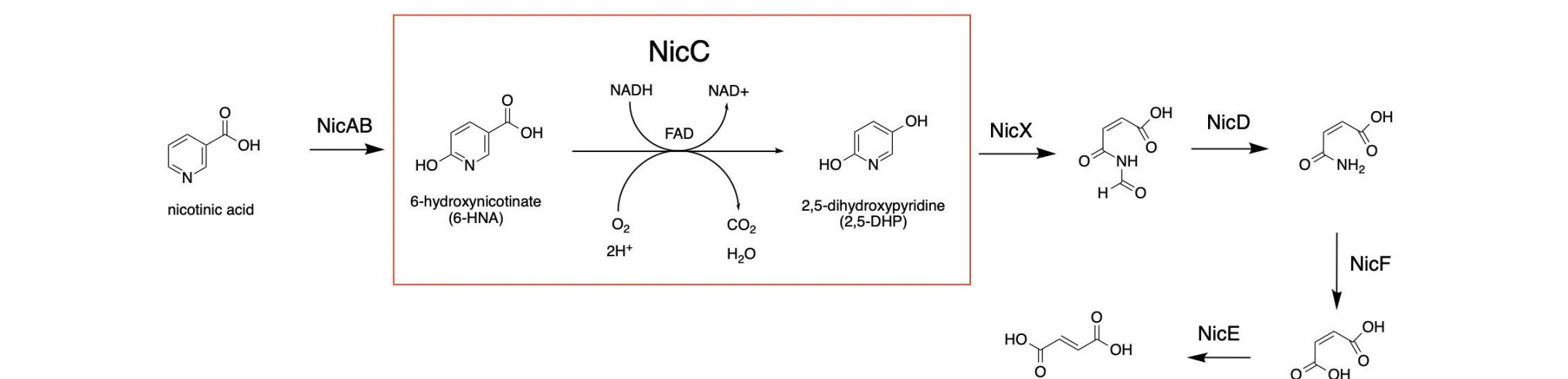


Figure 2. The degradation pathway of nicotinic acid (NA) leads to its conversion into fumaric acid, a central metabolic intermediate. nicC is emphasized as it facilitates the transformation of 6-hydroxynicotinate (6-HNA) to 2,5-dihydroxypyridine (2,5-DHP).

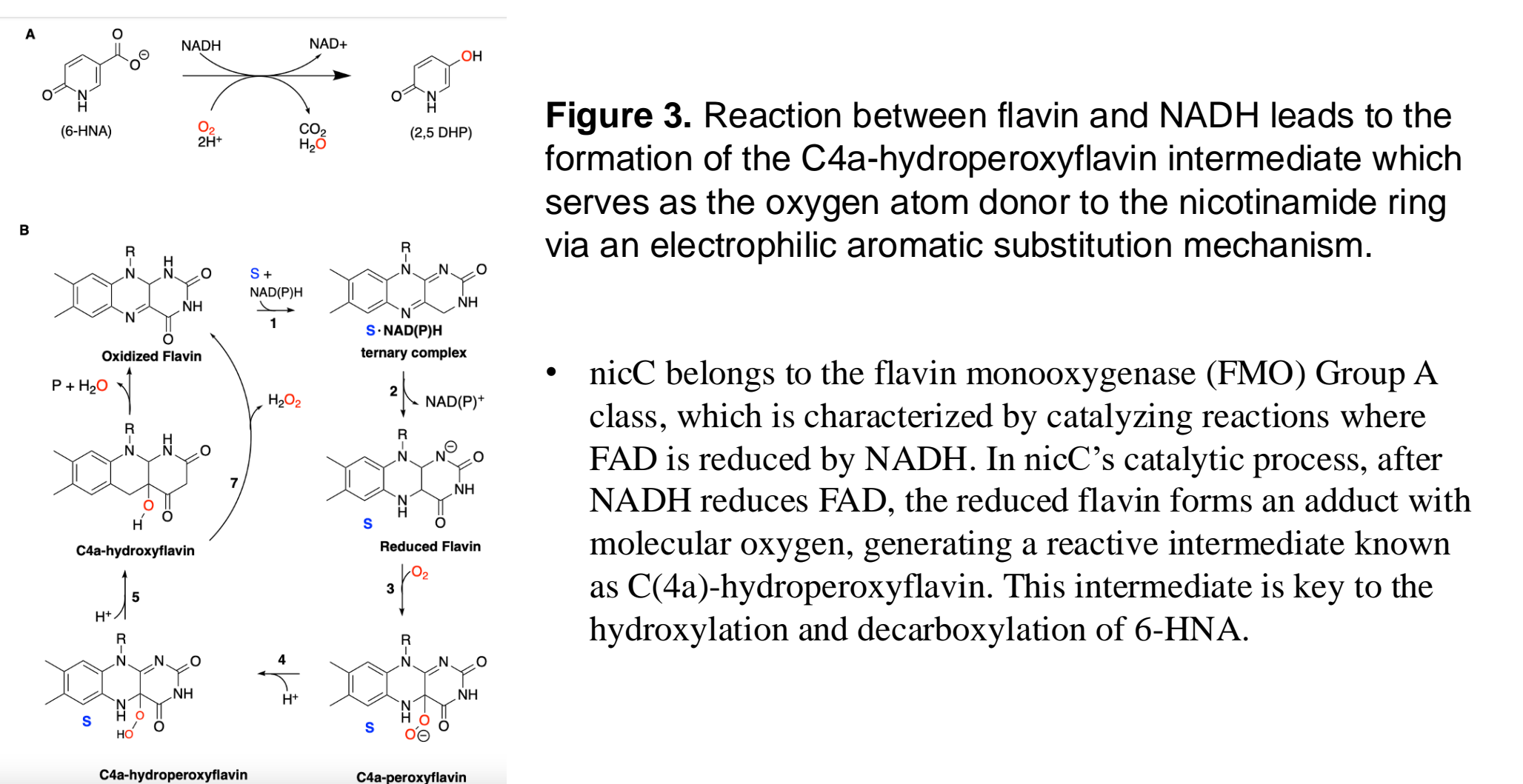


Figure 3. Reaction between flavin and NADH leads to the formation of the C(4a)-hydroperoxyflavin intermediate which serves as the oxygen atom donor to the nicotinamide ring via an electrophilic aromatic substitution mechanism.

- nicC belongs to the flavin monooxygenase (FMO) Group A class, which is characterized by catalyzing reactions where FAD is reduced by NADH. In nicC's catalytic process, after NADH reduces FAD, the reduced flavin forms an adduct with molecular oxygen, generating a reactive intermediate known as C(4a)-hydroperoxyflavin. This intermediate is key to the hydroxylation and decarboxylation of 6-HNA.

Hypothesis & Research Objectives

- Arg108 is positioned near the FAD-binding region and likely stabilizes the proper orientation of the flavin cofactor.
- NADH binds NicC at the FAD binding site.
- Arg 108 helps to facilitate this binding.
- Arg108 was subjected to site-directed mutagenesis, which generated the R108K lysine variant. In the absence of this stabilizing interaction, FAD may adopt a less favorable conformation for NADH binding, necessitating a higher concentration of NADH to achieve saturation and reducing the efficiency of hydride transfer.

R108K UV-Vis exhibits a decrease in NADH binding affinity and suggests substrate inhibition

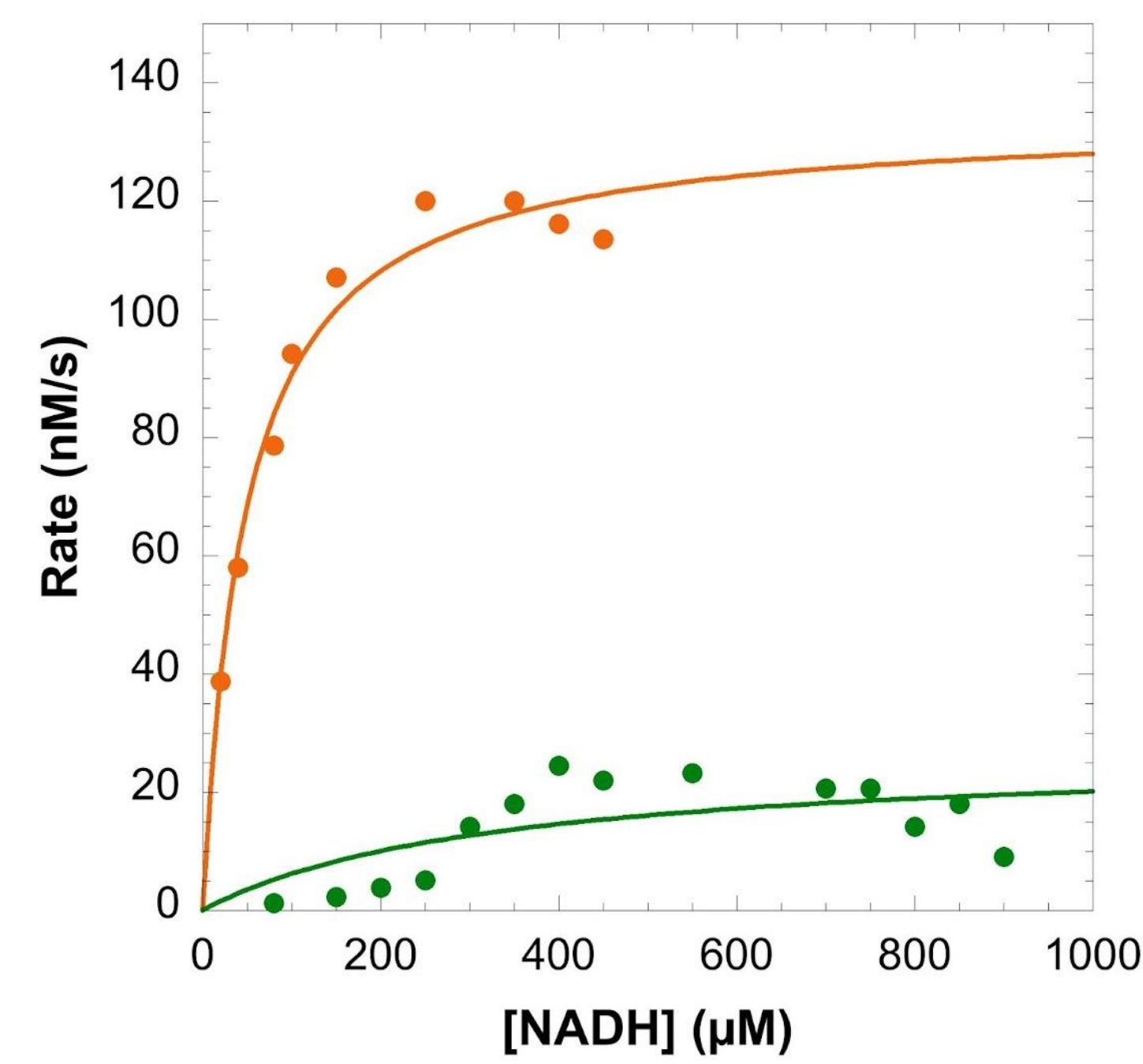


Figure 4. Steady-State Kinetics of the nicC R108K Variant at Two 6-HNA Concentrations by Following the Rate of NADH Oxidation at 340nm. The plot shows the reaction rate (nM/s) as a function of NADH concentration (μM) for the nicC R108K variant, with rates measured at 7500 μM (orange curve) and 500 μM (green curve) 6-HNA. The data were fitted to the Michaelis-Menten equation. The orange curve was repeated to determine whether the observed trend at higher NADH concentrations indicates potential substrate inhibition.

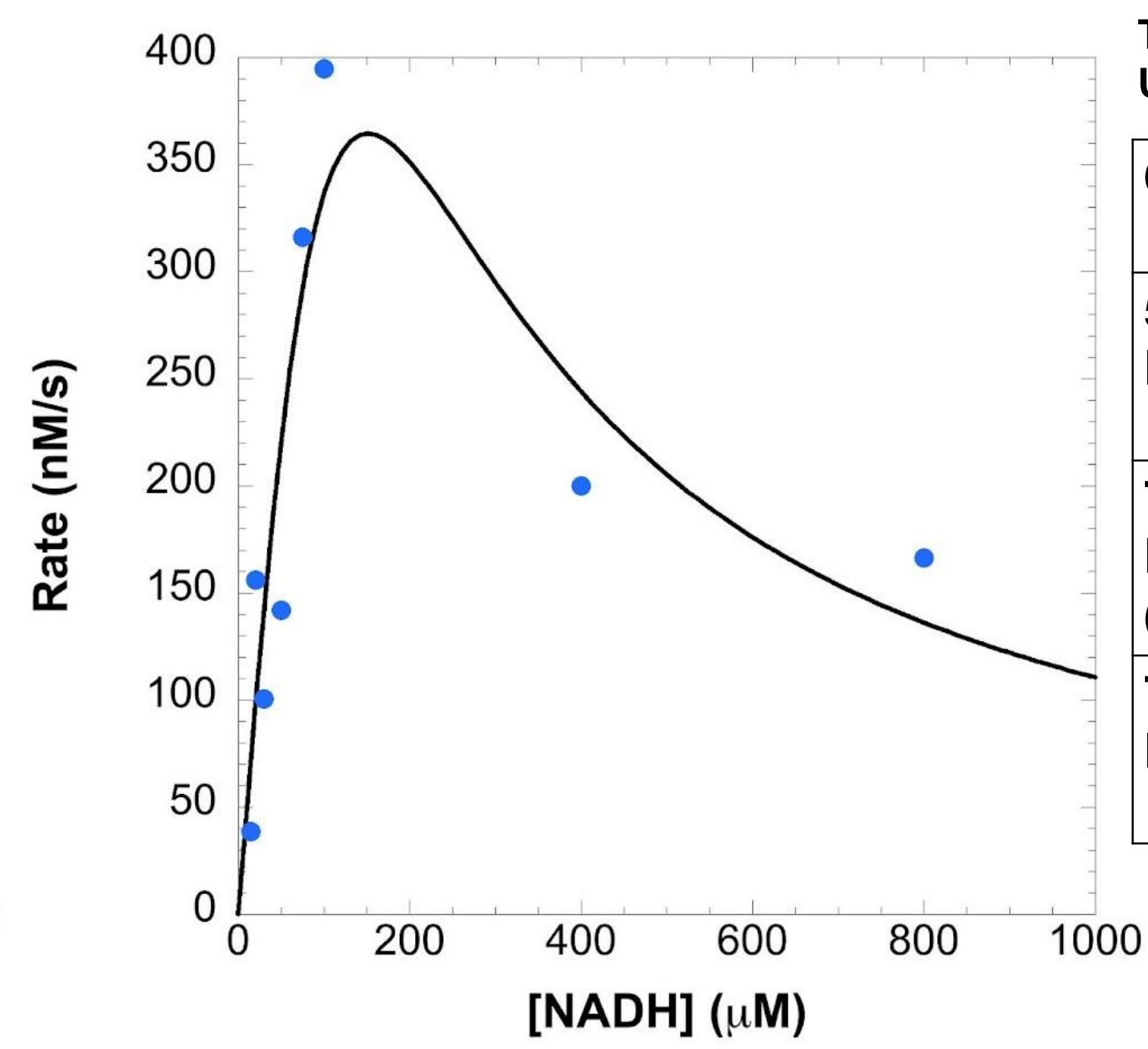


Figure 5. Steady-State Kinetics Using Substrate Inhibition Model of the nicC R108K Variant at 340 nm. The plot depicts the reaction rate (nM/s) as a function of NADH concentration (μM) for the nicC R108K variant in the presence of 7500 μM 6-HNA and 1 μM enzyme. The data exhibit a substrate inhibition trend, where the reaction rate increases at lower NADH concentrations but declines at higher levels. The curve is fitted to a non-linear regression fit to a non-linear regression model. The K_m of the fitted plot was derived to be $42 \pm 17 \mu\text{M}$, with a k_{cat} of 0.4 s^{-1} and a K_i of $665 \pm 430 \mu\text{M}$.

Table 1. Kinetic Parameters Derived from Michaelis-Menten Fits of UV-Vis Kinetics.

6-HNA (μM)	K_m (μM)	V_{max} (nM/s)	k_{cat} (s^{-1})
500 μM 6-HNA (Green)	335 ± 320	27 ± 10	0.03 ± 0.01
7500 μM 6-HNA (Orange)	50 ± 6	135 ± 5	0.13 ± 0.05
7500 μM 6-HNA (Blue)	42 ± 17	400 ± 0	665 ± 430

- Data in Table 1 demonstrate a clear dependence of enzyme activity on 6-HNA concentration

- As the higher concentration (7500 μM) yields a greater maximum velocity (V_{max}) and lower apparent K_m , indicative of more efficient catalysis under saturating substrate conditions.

- The dataset at 500 μM 6-HNA (green curve) exhibits significantly lower enzymatic activity, reflected by a much lower V_{max} and a higher K_m , suggesting that substrate availability is limiting enzyme function at this concentration.

R108K ITC reinforces a decrease in NADH binding affinity

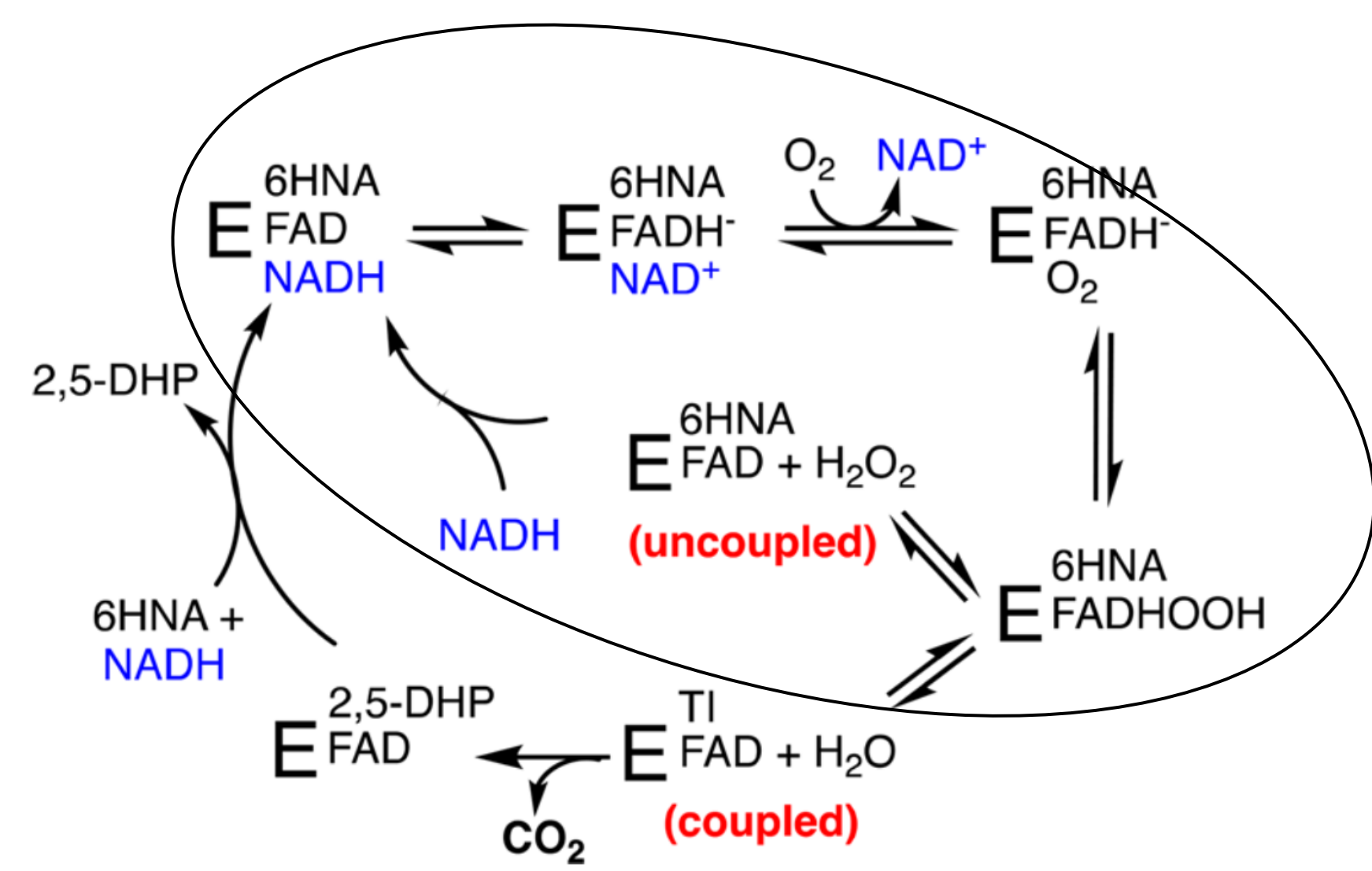


Figure 6. Schematic representation of NicC catalyzed reaction³.

- The R108K variant exhibited 53% coupling and 47% uncoupling.
- This helped to elucidate findings from ITC steady-state kinetics.

Table 2. Steady-State Kinetic Parameters for nicC R108K at Varying 6-HNA Concentrations.

6-HNA (μM)	k_{cat} (s^{-1})	K_m (mM)	k_{cat}/K_m	[Enzyme] μM
100	$(5.3 \pm 0.4) \times 10^{-2}$	$(1.2 \pm 0.1) \times 10^{-1}$	$(4.4 \pm 0.2) \times 10^{-2}$	4.5
250	$(5.3 \pm 0.3) \times 10^{-2}$	$(5.8 \pm 1) \times 10^{-2}$	$(9.1 \pm 0.8) \times 10^{-2}$	4
500	$(8.4 \pm 0.5) \times 10^{-2}$	$(5.7 \pm 0.9) \times 10^{-2}$	0.15 ± 0.02	3.5
1000	$(1.3 \pm 0.7) \times 10^{-2}$	$(5.4 \pm 0.9) \times 10^{-2}$	0.23 ± 0.05	3
2500	$(1.1 \pm 0.1) \times 10^{-2}$	$(3.9 \pm 1) \times 10^{-2}$	0.28 ± 0.08	2.5
5000	$(1.9 \pm 0.1) \times 10^{-2}$	$(3.9 \pm 0.8) \times 10^{-2}$	0.5 ± 0.2	2
7500	$(3.9 \pm 0.3) \times 10^{-2}$	$(5.2 \pm 1) \times 10^{-2}$	0.74 ± 0.5	2
10000	$(3.4 \pm 0.1) \times 10^{-2}$	$(4.2 \pm 0.5) \times 10^{-2}$	0.81 ± 0.6	2
12500	$(7.9 \pm 0.3) \times 10^{-2}$	$(1.1 \pm 0.1) \times 10^{-1}$	0.71 ± 0.5	1.5
15000	$(3.5 \pm 0.3) \times 10^{-2}$	$(5.1 \pm 1) \times 10^{-2}$	0.69 ± 0.5	1

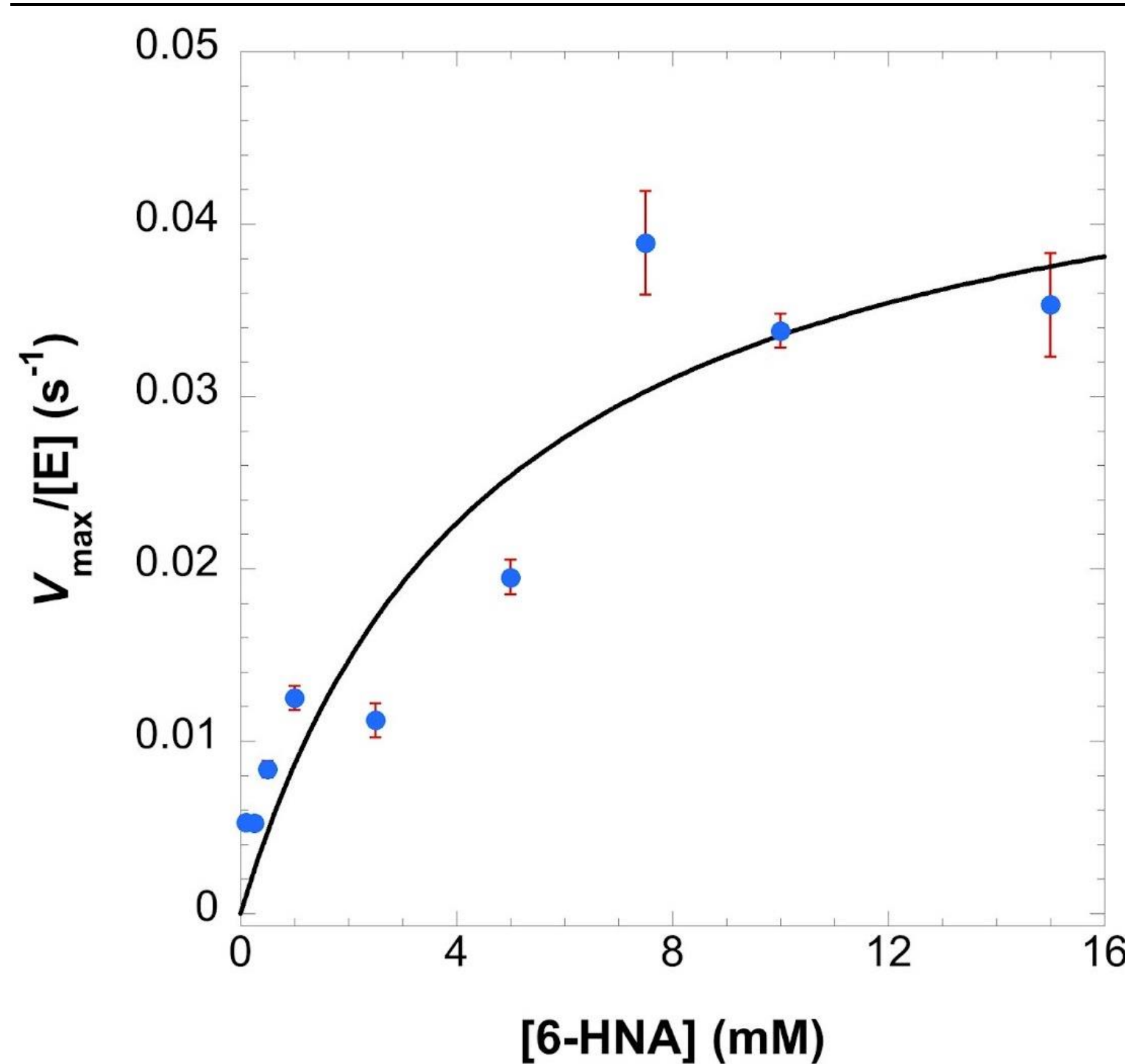


Figure 7. Figure 18. Re-Plot Showing Dependence of V_{max} on [6-HNA] for R108K nicC.

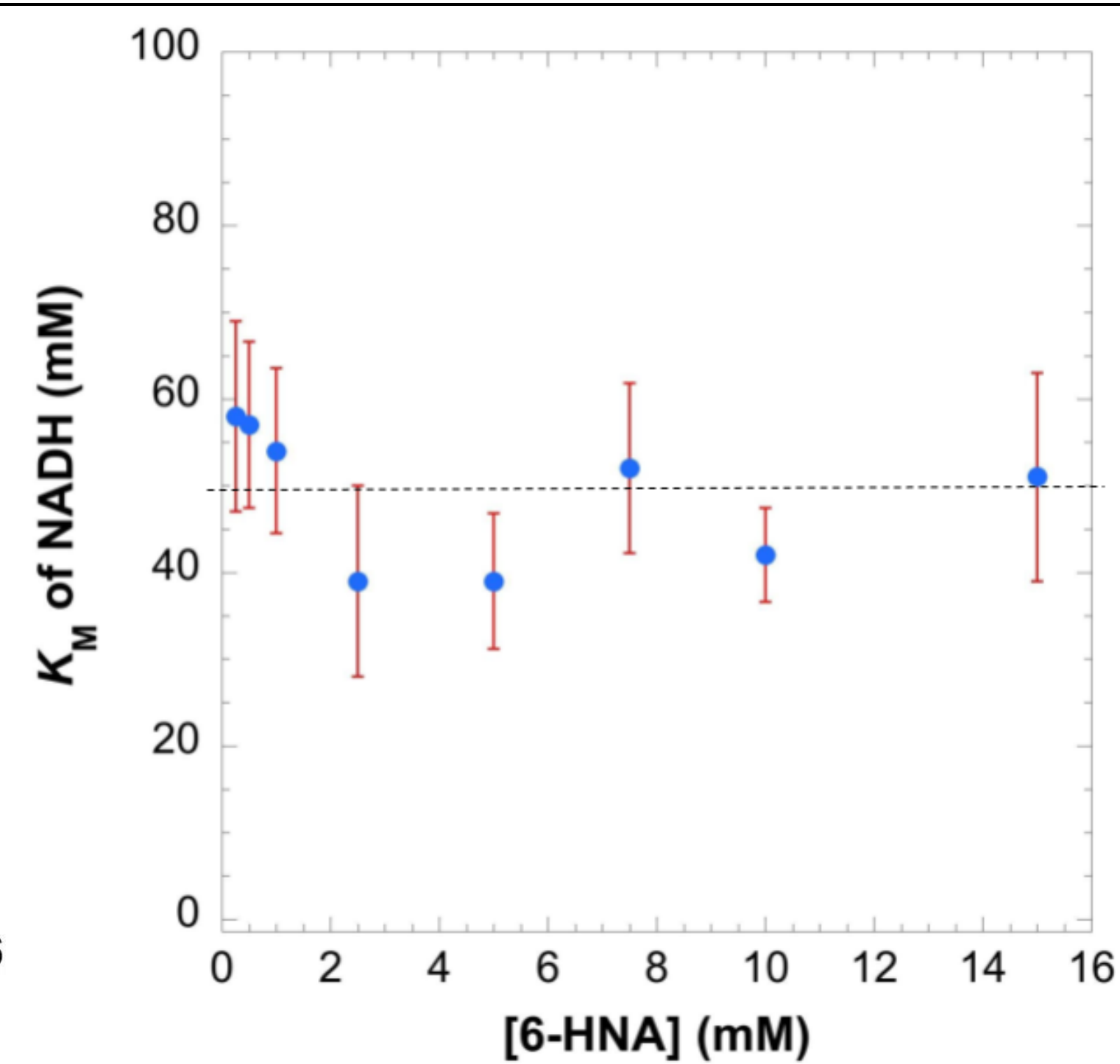


Figure 8. Re-Plot of Negligible Effect of 6-HNA on R108K nicC K_m for NADH.

- Figure 8 depicts the regression analysis follows a non-linear fit to the Michaelis-Menten equation, allowing for the determination of kinetic parameters.
- Notably, the K_m for 6-HNA was $5 \pm 3 \text{ mM}$, which is significantly higher than the wild-type value of $97 \pm 12 \mu\text{M}$, suggesting a substantial reduction in substrate affinity in the R108K variant. Overall $k_{\text{cat}} = 0.05 \pm 0.01 \text{ s}^{-1}$ derived from Table 2.

- Figure 9 is a summary of K_m values obtained by ITC kinetic analysis. Data reported in Table 2 Overall $K_m = 50 \pm 14 \text{ mM}$.

Arg 108 Conclusions

Arg 108 is important to the binding of NADH by nicC at the FAD binding site.

- The replacement of Arg 108 with Lys alters electrostatic interactions and hydrogen bonding networks in the active site.

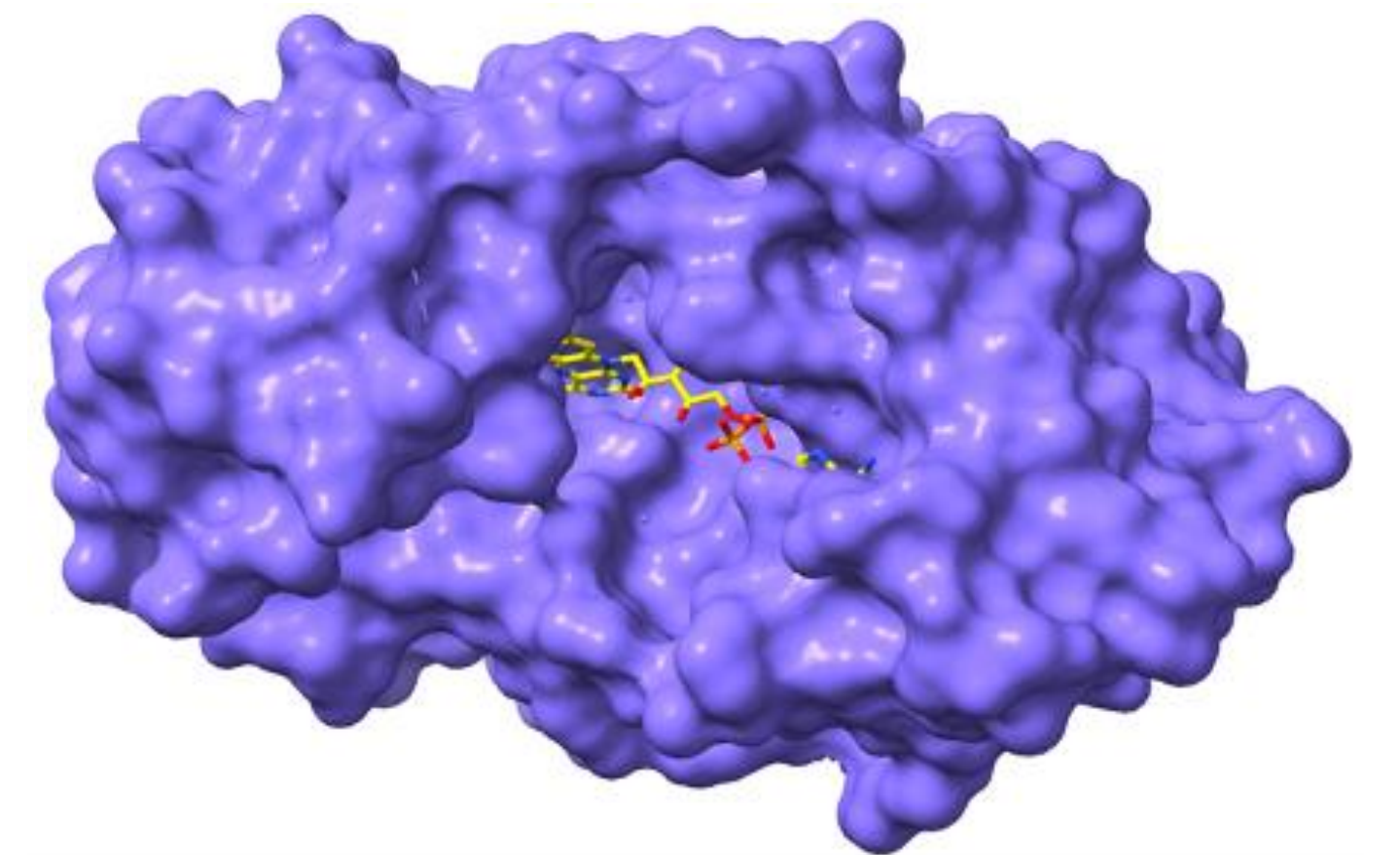
- NicC relies on NADH as an electron donor to reduce FAD, which then facilitates the hydroxylation reaction.

- The R108K mutation likely changes NADH positioning relative to FAD, leading to inefficient electron transfer.

Future Research

- Stopped-Flow Transient State Kinetics: Provide insight into the binding affinity of NADH by NicC (how tightly bound).

- Isolate reductive half-reaction to see how this variant affects hydride transfer without molecular oxygen.



- Investigate other residues within the FAD binding pocket.

- Accumulate research on multiple variants in this binding pocket to elucidate the binding of NADH by nicC.

Acknowledgements

- NSF Grant
- Copeland Funding
- Senior Independent Study

References

- Hirao, K., Shinohara, Y., Tsuda, H., Fukushima, S., and Takahashi, M. (1976) Carcinogenic Activity of Quinoline on Rat Liver. Cancer Research. U.S. National Library of Medicine.
- Pašková, V., Hilscherová, K., Feldmannová, M., and Bláha, L. (2006) Toxic effects and oxidative stress in higher plants exposed to polycyclic aromatic hydrocarbons and their N-Heterocyclic derivatives. Environmental Toxicology and Chemistry 25, 3238.
- Nakamoto, K. D.; Perkins, S. W.; Campbell, R. G.; Bauerle, M. R.; Gerwig, T. J.; Gerislioglu, S.; Wesdemiotis, C.; Anderson, M. A.; Hicks, K. A.; Snider, M. J. Mechanism of 6-Hydroxynicotinate 3-Monooxygenase, a Flavin-Dependent Decarboxylative Hydroxylase Involved in Bacterial Nicotinic Acid Degradation. Biochemistry 2019, 58 (13), 1751–1763.